Original Contribution

Staging Hemodynamic Failure With Blood Oxygen-Level–Dependent Functional Magnetic Resonance Imaging Cerebrovascular Reactivity

A Comparison Versus Gold Standard (^{15}O-)H_2O-Positron Emission Tomography

Jorn Fierstra, MD, PhD; Christiaan van Niftrik, MD; Geoffrey Warnock, PhD; Susanne Wegener, MD; Marco Piccirelli, PhD; Athina Pangalu, MD; Giuseppe Esposito, MD, PhD; Antonios Valavanis, MD; Alfred Buck, MD; Andreas Luft, MD; Oliver Bozinov, MD; Luca Regli, MD

Background and Purpose—Increased stroke risk correlates with hemodynamic failure, which can be assessed with (^{15}O-)H_2O positron emission tomography (PET) cerebral blood flow (CBF) measurements. This gold standard technique, however, is not established for routine clinical imaging. Standardized blood oxygen-level–dependent (BOLD) functional magnetic resonance imaging+CO_2 is a noninvasive and potentially widely applicable tool to assess whole-brain quantitative cerebrovascular reactivity (CVR). We examined the agreement between the 2 imaging modalities and hypothesized that quantitative CVR can be a surrogate imaging marker to assess hemodynamic failure.

Methods—Nineteen data sets of subjects with chronic cerebrovascular steno-occlusive disease (age, 60±11 years; 4 women) and unilaterally impaired perfusion reserve on Diamox-challenged (^{15}O-)H_2O PET were studied and compared with a standardized BOLD functional magnetic resonance imaging+CO_2 examination within 6 weeks (8±19 days). Agreement between quantitative CBF- and CVR-based perfusion reserve was assessed. Hemodynamic failure was staged according to PET findings: stage 0: normal CBF, normal perfusion reserve; stage I: normal CBF, decreased perfusion reserve; and stage II: decreased CBF, decreased perfusion reserve. The BOLD CVR data set of the same subjects was then matched to the corresponding stage of hemodynamic failure.

Results—PET-based stage I versus stage II could also be clearly separated with BOLD CVR measurements (CVR for stage I 0.11 versus CVR for stage II −0.03; $P<0.01$). Hemispheric and middle cerebral artery territory difference analyses (ie, affected versus unaffected side) showed a significant correlation for CVR impairment in the affected hemisphere and middle cerebral artery territory ($P<0.01$, $R^2=0.47$ and $P=0.02$, $R^2= 0.25$, respectively).

Conclusions—BOLD CVR corresponded well to CBF perfusion reserve measurements obtained with (^{15}O-)H_2O-PET, especially for detecting hemodynamic failure in the affected hemisphere and middle cerebral artery territory and for identifying hemodynamic failure stage II. BOLD CVR may, therefore, be considered for prospective studies assessing stroke risk in patients with chronic cerebrovascular steno-occlusive disease, in particular because it can potentially be implemented in routine clinical imaging. **(*Stroke*. 2018;49:00-00. DOI: 10.1161/STROKEAHA.117.020010.)**

Key Words: brain ■ cerebrovascular disorders ■ hemodynamics ■ magnetic resonance imaging ■ middle cerebral artery

Downloaded from http://stroke.ahajournals.org/ by guest on July 19, 2018

Various cerebral hemodynamic parameters derived from computed tomography (CT) and magnetic resonance imaging (MRI)–based techniques have been associated with increased stroke risk in patients with chronic cerebrovascular steno-occlusive disease.[1–7] Among all these parameters, such as cerebrovascular reactivity (CVR), mean transit time, cerebral blood volume, oxygen extraction fraction, cerebral metabolic rate of oxygen, the gold standard remains direct cerebral blood flow (CBF) measurements that can be generated with (^{15}O-)H_2O-positron emission tomography (PET). By applying an acetazolamide (=Diamox) challenge during a second scan, the degree of hemodynamic failure can be

Received August 14, 2017; final revision received November 3, 2017; accepted November 29, 2017.

From the Departments of Neurosurgery (J.F., C.v.N., G.E., O.B., L.R.), Neuroradiology (M.P., A.V.), Neurology (S.W., A.L.), Pharmacology and Toxicology (G.W.), and Nuclear Medicine (A.B.), Clinical Neuroscience Center, University Hospital Zurich, University of Zurich, Switzerland.

The online-only Data Supplement is available with this article at http://stroke.ahajournals.org/lookup/suppl/doi:10.1161/STROKEAHA.117.020010/-/DC1.

Correspondence to Jorn Fierstra, MD, PhD, Department of Neurosurgery, University Hospital Zurich, Frauenklinikstrasse 10, 8091 Zurich, Switzerland. E-mail jorn.fierstra@usz.ch

© 2018 American Heart Association, Inc.

estimated (ie, perfusion reserve). Hemodynamic failure has been described as follows: stage 0: normal CBF and normal perfusion reserve; stage I: normal CBF, decreased perfusion reserve; and stage II: decreased CBF and decreased perfusion reserve, where hemodynamic failure stage II has been associated with the highest stroke risk.[1–3] Although efforts have been made to streamline the (^{15}O-)H_2O-PET examination for routine clinical practice, that is, noninvasive measurements without a direct arterial input function,[8] it remains only available in few specialized centers and requires a radioactive tracer.

Quantitative CVR measurements derived from blood oxygen-level–dependent (BOLD) functional MRI (fMRI)[9,10] may be applied as a novel imaging marker for hemodynamic failure, in particular because it is a brief single acquisition and can potentially be implemented on every clinical MRI system.[11] In this case, CVR is the percentage change in BOLD signal per mm Hg change in CO_2 and can be used as an indicator of how much cerebrovascular reserve capacity is left in a given vascular bed. Reductions in CVR can range from a blunted increase in blood flow in mild cases to paradoxical reduction in regional blood flow indicating steal phenomenon in severe cases.

Because quantitative CVR derived from BOLD fMRI is only an indirect measurement of perfusion reserve, we studied patients with chronic cerebrovascular steno-occlusive disease exhibiting unilateral hemodynamic failure that had undergone both a Diamox-challenged (^{15}O-)H_2O-PET examination (considered the gold standard) and a standardized BOLD fMRI+CO_2 examination within 6 weeks to assess the use of quantitative CVR as a surrogate imaging marker for hemodynamic failure.

Methods

Data Selection

Requests to access the analysis methods and detailed results of this study may be sent to the corresponding author (Dr Fierstra). Study approval was obtained by the cantonal ethics board of Zurich, Switzerland (KEK-ZH-Nr. 2012-0427), and all subjects signed informed consent before study participation. Nineteen data sets of 16 patients with chronic cerebrovascular steno-occlusive disease were selected based on the following inclusion criteria: unilateral perfusion impairment on the clinical (^{15}O-)H_2O-PET examination as determined by an experienced nuclear radiologist (A.B.). Eligible patients were then matched to our prospective BOLD fMRI CVR database, and those subjects with a maximum time period of 6 weeks between both examinations (ie, (^{15}O-)H_2O-PET and BOLD fMRI CVR study) were selected for further data analysis. In addition, 10 age-matched healthy subjects were included. Exclusion criteria were age <18 years old and patients with new neurological events or neurosurgical/neurointerventional procedures between both scans.

PET Protocol

PET data were acquired on a full ring PET/CT-scanner in 3-dimensional mode (PET/CT Discovery STE, GE Healthcare, Waukesha, MI) and corrected for attenuation and scatter by using the corresponding CT (120 kV/80 mA) and manufacturer's algorithms. The scanner's axial field of view covered 15.3 cm. Three hundred to 800 MBq (^{15}O-)H_2O was administered intravenously using an automatic injection device. The tracer was delivered for 20 seconds. The emission data were acquired as a series of 18, 10-second frames. Baseline and Diamox scans were each performed using the same protocol, with at least 15 minutes between tracer injections. Diamox was injected 13 minutes before the second PET scan, with dose adjusted according to subjects' weight and injection time for 2 minutes. Images were reconstructed using a 3-dimensional Fourier rebinning filtered back projection algorithm resulting in a 128×128×47 matrix with 2.34×2.34×3.27 mm voxel spacing. Parametric images of CBF were generated using a previously reported method[8,12] in which a standardized arterial input function and image scaling based on the washout rate k2 of (^{15}O-)H_2O are used to determine CBF, defined as mL/100 mg per minute. This method described by Treyer et al[8] uses the fact that k2 is related to the shape and not the scale of the arterial input function and proportional to CBF. A total count-rate threshold was set at 50% of the max.

PET Processing

The baseline and Diamox PET images were coregistered to the mean BOLD volume. Normalization of the 2 PET images was done into Montreal Neurological Institute space, and both images were smoothed with a Gaussian Kernel with 8-mm full width at half maximal.

Quantitative PET perfusion reserve data were calculated as follows:

$$\text{PET perfusion reserve} = \frac{\text{Diamox PET} - \text{Baseline PET}}{\text{Baseline PET}}$$

PET perfusion reserve was defined as the percent CBF change during a Diamox challenge.

MRI Protocol

BOLD volumes were obtained on a 3-Tesla Skyra VD13 (Siemens, Erlangen, Germany) with a 32-channel head coil. An axial 2-dimensional echo planar imaging BOLD fMRI sequence was planned on the anterior commissure–posterior commissure line plus 20° on a sagittal image with voxel size 3×3×3 mm^3, acquisition of matrix 64×64×35 slices with ascending interleaved acquisition, slice gap 0.3 mm, Generalized Autocalibrating Partial Parallel Acquisition (GRAPPA) factor 2 with 32 ref. lines, repetition time/echo time 2000/30 ms, flip angle 85°, bandwidth 2368 Hz/Px, and field of view 192×192mm. In addition, a high-resolution 3-dimensional T1-weighted image with the same orientation as the fMRI scans was obtained for coregistration and overlay of the CVR map. The acquisition parameters were voxel size 0.8×0.8×1.0 mm with a field of view 230×230 mm and resolution of 288×288, 176 slices per slab with a thickness of 1 mm, repetition time/echo time 2200/5.14 ms, inversion time 900 ms, and flip angle 8°.

By using a custom-build computer-controlled gas blender (RepirAct, Thornhill Research Institute, Toronto, Canada) containing the prospective gas targeting algorithms of Slessarev et al,[13] precise control of partial pressure of end-tidal CO_2 and partial pressure of end-tidal O_2 could be achieved. Advances of this novel CO_2/O_2 control as compared with other vasoactive methods have been described in greater detail previously.[9,10] BOLD signal changes were induced by a single hypercapnia pseudo square wave. The pseudo square wave consisted of a hypercapnia plateau of 50 mm Hg CO_2, from a preset baseline of 40 mm Hg, for 80 seconds preceded and followed by a 100-second baseline of 40 mm Hg CO_2. During the entire protocol, iso-oxia (PO_2 100 mm Hg) was maintained.

BOLD CVR Post-Processing

BOLD data sets were slice-time corrected and realigned for motion correction. Subjects with motion >3 mm in any direction were excluded for further analysis. In accordance to the PET data sets, the BOLD images were normalized to Montreal Neurological Institute space and smoothed with a Gaussian Kernel with 8-mm full width at half maximal. After temporal shifting for optimal physiological correlation of the 2 time series, CVR was calculated from the slope of a linear least square fit of the BOLD signal time course to the CO_2 time series over the range of the first baseline of 100 seconds, the step portion of the protocol and the second baseline of 100 seconds on a voxel-by-voxel basis. CVR was defined as the percentage BOLD signal change/mm Hg CO_2.[14] The extra BOLD volumes were acquired to allow for potential temporal shift (for more information, see van Niftrik et al[14]).

Downloaded from http://stroke.ahajournals.org/ by guest on July 19, 2018

Table 1. Baseline Characteristics

Study No.	Age	Sex	Diagnosis	Vascular Risk Factors	Angiographic Findings*	Anatomic MRI Findings	Time Period Between Scans, d	Hemodynamic Failure Stage†
1a	50	M	Carotid atherosclerosis	Smoking, hypercholesteremia, hypertension	Right ICA occlusion	Ischemia semioval center and globus pallidus right	31	2
1b					Contralateral ICA no stenosis patent Acom		28	2
2a	58	M	Carotid atherosclerosis	Smoking, hypertension	Right ICA occlusion, no stenosis contralateral ICA, patent Acom and Pcom right	Watershed infarctions between right ACA-MCA territory	3	1
2b							28	2
3a	80	M	Carotid atherosclerosis	Smoking, hypertension, positive family history	Right ICA occlusion, no contralateral ICA stenosis, retrograde filling ophthalmic artery right	Chronic ischemia signs in MCA territory right	40	2
3b							37	1
4	77	M	Carotid atherosclerosis	Hypercholesteremia, hypertension	Left ICA occlusion, 40% ICA stenosis right, patent Acom	Multiple small infarctions in left MCA territory	8	1
5	46	M	Carotid atherosclerosis	Hypertension, smoking, hypercholesteremia	Right ICA stenosis 90%, left ICA stenosis 50%, patent Pcom ipsilateral, patent Acom	Multiple small infarctions in right MCA territory	18	1
6	51	F	Moya-Moya disease	Hypertension	Bilateral M1 occlusion	Chronic ischemia in right MCA territory	26	1
7	66	F	Sphenoid wing meningioma	Hypercholesteremia	Left ICA occlusion, no contralateral ICA stenosis, patent Acom, and Pcom bilaterally	Subacute small infarctions left MCA territory	5	1
8	51	M	Carotid atherosclerosis	Smoking	Left ICA occlusion, no contralateral ICA stenosis	Subacute small infarctions in MCA territory left	38	1
9	64	M	Carotid atherosclerosis	Hypertension, smoking	Right ICA occlusion, 30% left ICA stenosis. Patent Acom. Patent ipsilateral Pcom	No signs of ischemia	19	1
10	44	F	Moya-Moya disease	None	Bilateral MCA/ACA stenosis	No signs of ischemia	4	1
11	62	F	Carotid atherosclerosis	Smoking, hypertension, hypercholesteremia, positive family history	Left ICA occlusion, 50% stenosis contralateral ICA. Patent Acom+Pcom bilateral	Small cortical infarctions in left MCA territory	4	2
12	68	M	Carotid atherosclerosis	Smoking hypertension, hypercholesteremia	Right ICA occlusion, 80% stenosis contralateral ICA. Patent Acom+Pcom bilateral	Multiple infarctions in right basalganglia	9	2
13	76	M	Carotid atherosclerosis	Smoking hypertension, hypercholesteremia	Bilateral ICA occlusion, patent Pcom bilateral	Subacute multiple ischemia in right semioval center	24	1
14	64	M	Carotid atherosclerosis	Hypertension, diabetes mellitus, smoking	Right ICA occlusion, 40% contralateral ICA stenosis. Patent right Pcom	Leukoaraiosis in right semioval center	6	2

(*Continued*)

Downloaded from http://stroke.ahajournals.org/ by guest on July 19, 2018

Stroke

Table 1. Continued

Study No.	Age	Sex	Diagnosis	Vascular Risk Factors	Angiographic Findings*	Anatomic MRI Findings	Time Period Between Scans, d	Hemodynamic Failure Stage†
15	47	M	Carotid atherosclerosis	None	Right M1 occlusion, no contralateral ICA stenosis	Multiple subacute infarctions in right MCA territory	10	2
16	52	M	Carotid atherosclerosis	Smoking, diabetes mellitus	Left ICA occlusion, 60% stenosis contralateral ICA. Patent Acom	Multiple chronic infarctions in left MCA territory	5	1

ACA indicates anterior cerebral artery; Acom, anterior communicating artery; F, female; ICA, internal carotid artery; M, male; M1, middle cerebral artery 1 segment; M2, middle cerebral artery 2 segment; MCA, middle cerebral artery; MRI, magnetic resonance imaging; and Pcom, posterior communicating artery.

*ICA stenosis graded according to NASCET criteria (North American Symptomatic Carotid Endarterectomy Trial).

†Hemodynamic staging is given for the affected hemisphere because the inclusion criteria was unilateral hemodynamic failure determined with positron emission tomography.

Vascular Territory Analysis and Staging of Hemodynamic Failure

Quantitative BOLD CVR and PET perfusion reserve values of the middle cerebral artery (MCA) vascular territory were determined by applying a vascular atlas derived from predefined brain regions from the standard N30R83 atlas by Hammers et al[15] and Kuhn et al[7] to the normalized CVR maps. An independent experienced nuclear radiologist assessed all PET images for staging hemodynamic failure (A.B.). In particular, baseline PET and Diamox PET were assessed for reduction in perfusion to divide MCA flow territories per patient into 3 groups:

- Stage 0: normal baseline CBF and normal perfusion reserve after Diamox challenge
- Stage I: normal baseline CBF with decreased perfusion reserve after Diamox challenge
- Stage II: decreased baseline CBF and decreased perfusion reserve after Diamox challenge

Quantitative Analysis

All statistical analysis was done using the software SPSS 23 (IBM SPSS Statistical 23). To assess the correlation between quantitative BOLD and PET for the whole brain, both hemispheres as well as for the MCA flow territory, a Pearson correlation coefficient was obtained ($P \leq 0.05$ is significant). A difference analysis for both modalities was done by subtracting the mean value of the affected hemisphere from the unaffected hemisphere. An unpaired *t* test was used to compare BOLD CVR and PET perfusion reserve values within the MCA flow territory between the 3 aforementioned groups. Additional analyses were done to determine test accuracy (receiver operating characteristic curve) and limits of agreement between the 2 techniques (Bland–Altman).

Results

Nineteen data sets from 16 subjects (age, 60±11 years; 4 women) and 10 age-matched healthy subjects (age, 59±5 years; 4 women, 6 men) were included for the analysis. The mean time between the 2 scans was 8±19 days. Three subjects had undergone a (^{15}O-) H_2O-PET examination twice over time (as part of routine follow-up imaging) and matched the inclusion criteria of an additional BOLD CVR examination within 6 weeks. Further subject information is given in Table 1. Figure 1 shows an illustrative PET and BOLD image of a subject with right-sided internal carotid artery occlusion and corresponding hemodynamic impairment of the right hemisphere (stage II). Illustrative movies of whole brain BOLD CVR and PET perfusion reserve measurements of the same subject are given in the online-only Data Supplement.

BOLD CVR Versus PET Perfusion Reserve Findings

An overview of PET perfusion reserve measurements and BOLD CVR findings are presented in Table 2. Quantitative BOLD CVR findings were significantly lower in patients when compared with the healthy cohort (0.11±0.07 versus 0.23±0.03; $P<0.01$). In healthy subjects, the CVR values of the left and right hemisphere did not differ from each other. These values, however, were significantly higher than the CVR of both the affected, as well as—interestingly—the unaffected, hemisphere of patients ($P<0.01$). Significant differences between the affected and unaffected hemisphere were found for both BOLD and PET: BOLD CVR affected hemisphere versus unaffected hemisphere 0.08 versus 0.15, $P<0.01$; PET perfusion reserve affected hemisphere versus unaffected hemisphere 0.33 versus 0.47, $P<0.01$. This could also be seen for the MCA flow territory of the affected versus unaffected hemisphere (BOLD CVR: 0.04 versus 0.15, $P<0.01$; PET perfusion reserve: 0.19 versus 0.44, $P<0.01$). When considering exclusively the quantitative values of BOLD CVR and PET perfusion reserve for whole brain, unaffected and affected hemisphere, no significance was found (whole brain: $R^2=0.03$, $P=0.82$; unaffected hemisphere: $R^2=0.01$, $P=0.83$; affected hemisphere: $R^2=0.26$, $P=0.51$; Figure 2A). The MCA territory, however, showed an agreement although weak ($P=0.02$; $R^2=0.25$; Figure 2B). Interestingly, after subtracting the values of the affected hemisphere from the unaffected hemisphere (ie, a difference analysis), a significant correlation was found for the hemispheric difference ($P<0.01$; $R^2=0.47$; Figure 2C), as well as for the MCA territory ($P<0.01$; $R^2=0.61$; Figure 2D).

Staging Hemodynamic Failure With BOLD CVR Versus PET Perfusion Reserve

Finally, the agreement between BOLD CVR versus PET-derived perfusion reserve for staging hemodynamic failure in the MCA territory was assessed. The staging was determined based on the PET scan by an experienced nuclear radiologist (A.B.), whereas the BOLD study of the same subject was then matched to that PET hemodynamic stage.

No significant difference was found between stage 0 and stage I for both examinations; however, BOLD CVR showed a trend toward more impairment for stage I (BOLD CVR stage 0 versus stage I: 0.15 versus 0.11, $P=0.07$; PET perfusion reserve

Downloaded from http://stroke.ahajournals.org/ by guest on July 19, 2018

Stroke

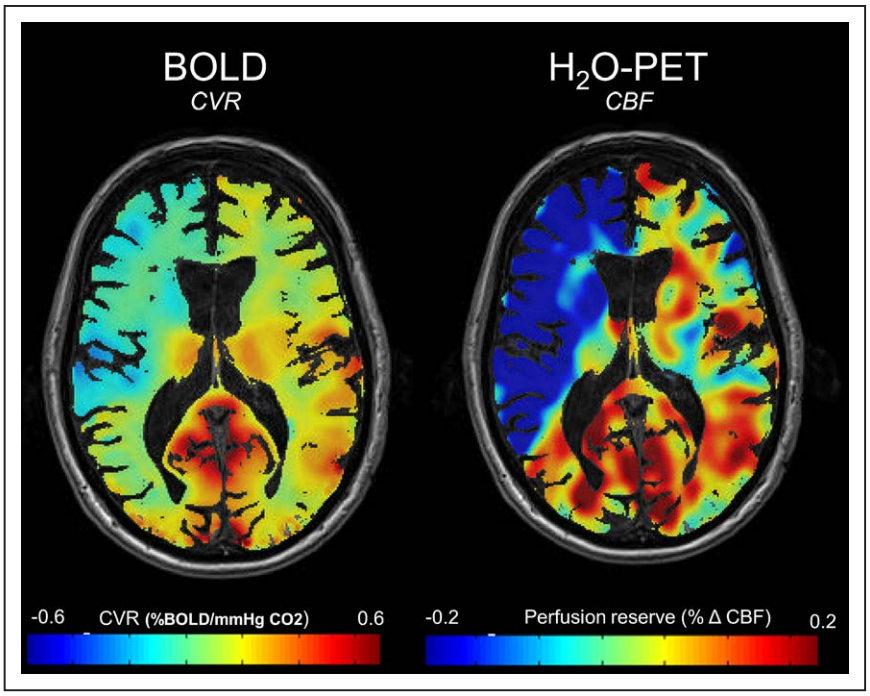

Figure 1. Blood oxygen-level–dependent (BOLD) cerebrovascular reactivity (CVR) map vs (^{15}O-)H_2O-positron emission tomography (PET) perfusion reserve map. Illustrative axial slide of (**A**) BOLD CVR and (**B**) Diamox-challenged (^{15}O-)H_2O-PET perfusion reserve map of a subject with right-sided carotid artery occlusion. Both maps demonstrate good spatial agreement in the right hemisphere exhibiting steal phenomenon, that is, hemodynamic failure stage II (depicted in blue). In addition, the BOLD CVR map also demonstrates CVR impairment in the contralateral unaffected hemisphere (green-yellow), something that is not apparent on the PET map. Both BOLD CVR and PET perfusion reserve are color coded ranging from steal phenomenon (blue) to normal (red) and superimposed on an anatomic underlay. Supporting movies of these 2 images are provided in the online-only Data Supplement illustrating both CVR and perfusion reserve for the entire brain. CBF indicates cerebral blood flow.

stage 0 versus stage I: 0.41 versus 0.34, P=0.46). PET-based stage II hemodynamic failure exhibited a significant impairment as compared with stage I for BOLD CVR (BOLD CVR stage I versus stage II: 0.11 versus −0.03; P<0.01). The PET perfusion reserve showed a weaker agreement (PET perfusion reserve stage I versus stage II: 0.34 versus 0.12; P=0.05). The mean values, distribution and agreement of BOLD CVR, and PET perfusion reserve findings for all 3 stages are presented in Figures 3 and 4.

Discussion

In this study, we compared 19 quantitative BOLD CVR data sets of patients with chronic cerebrovascular steno-occlusive disease against (^{15}O-)H_2O-PET perfusion reserve measurements and demonstrated that BOLD CVR can be used as a surrogate imaging marker for hemodynamic failure. With a good agreement between both techniques for determining hemodynamic failure of the affected hemisphere and MCA territory and for hemodynamic failure stage II, increased stroke risk for individual chronic cerebrovascular pathologies, such as carotid artery occlusion, may be studied in more detail in the future. Interestingly, we noted contralateral CVR impairment in the assumingly unaffected hemisphere in all 19 data sets, something that did not become apparent from PET perfusion reserve measurements. A likely explanation may be that CBF can still be maintained through vascular contributions from other sources, including the contralateral hemisphere within a certain degree of CVR impairment. This may implicate the presence of chronic tissue injury without apparent tissue loss on anatomic imaging (ie, cortical thinning).[16,17]

The agreement between quantitative BOLD CVR and PET perfusion reserve values was relatively weak, as could be expected. This becomes apparent in Figures 2 and 3 where the PET ranges are wide, whereas the BOLD CVR values were

Table 2. BOLD CVR and PET Perfusion Reserve Findings

	Patients				Healthies
	PET			BOLD	BOLD
	CBF Baseline	CBF Post-Diamox	Perfusion Reserve	CVR	CVR
Whole brain	25.4±8.5	33.4±8.4	0.41±0.40	0.11±0.07	0.23±0.03
Left hemisphere					0.24±0.03
Right hemisphere					0.22±0.04
Affected hemisphere	24.8±8.4	30.9±8.1	0.33±0.39	0.08±0.09	
Unaffected hemisphere	26.3±8.9	36.1±9.1	0.48±0.35	0.15±0.07	
MCA territory					
Affected hemisphere			0.19±0.25	0.04±0.09	
Unaffected hemisphere			0.44±0.21	0.15±0.10	

BOLD indicates blood oxygen-level–dependent; CBF, cerebral blood flow (mL/100 mg tissue per minute); CVR, cerebrovascular reactivity (%BOLD signal change/mm Hg CO_2); MCA, middle cerebral artery; and PET, position emission tomography.

Downloaded from http://stroke.ahajournals.org/ by guest on July 19, 2018

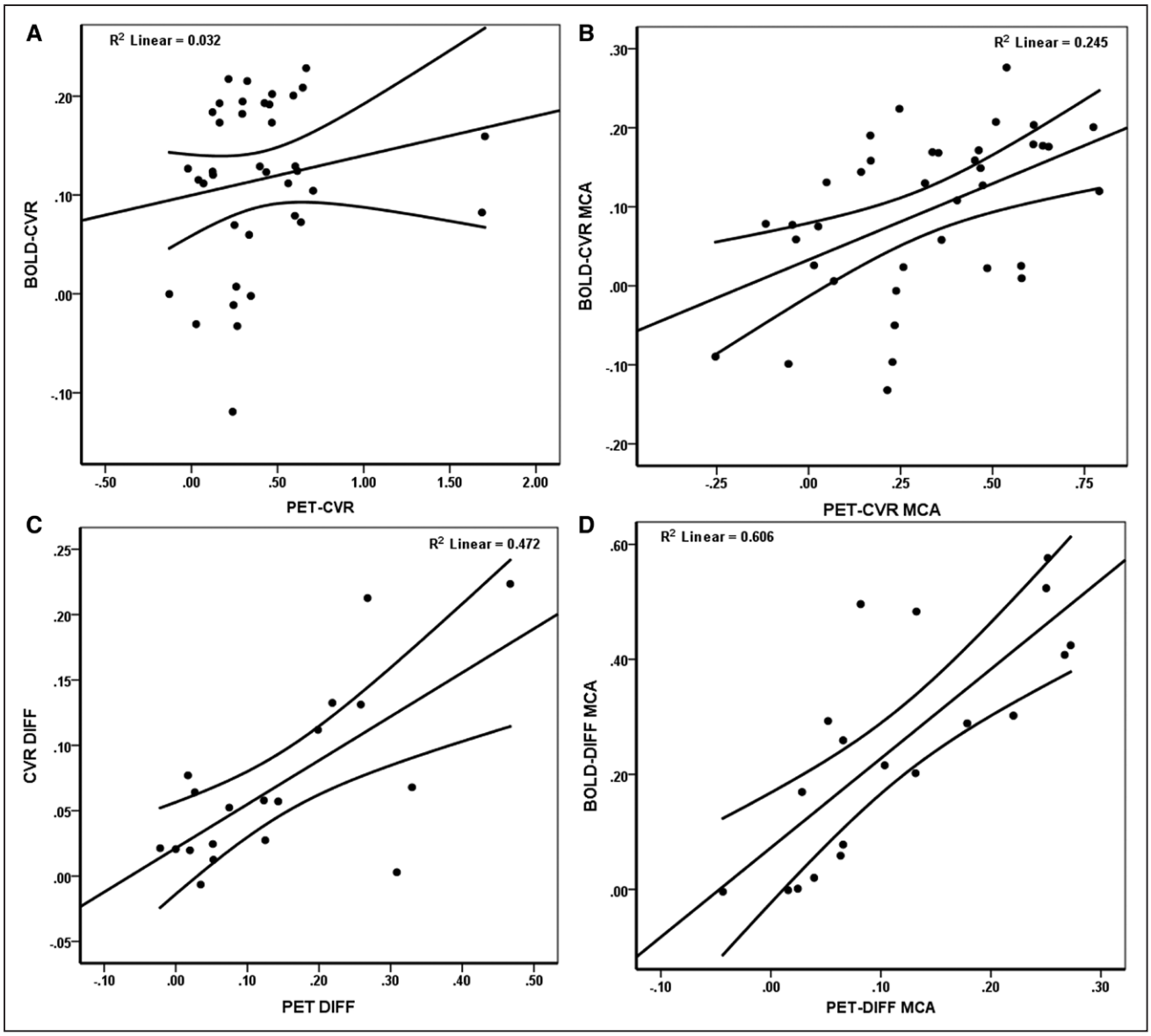

Figure 2. Correlation of blood oxygen-level–dependent (BOLD) cerebrovascular reactivity (CVR) values vs (^{15}O-)H_2O-positron emission tomography (PET) perfusion reserve values. Correlation of BOLD CVR and PET perfusion reserve for whole brain (**A**) and middle cerebral artery (MCA) territory (**B**). Correlation of the hemispheric difference analysis is given in (**C**) for whole brain and (**D**) MCA territory. DIFF indicates difference.

less scattered. Although the (^{15}O-)H_2O-PET method using a standardized arterial input function can produce actual CBF values, scaling errors may occur where the kinetics of the tracer in the blood do not fit the shape of the standardized curve, leading to a wide range or various thresholds for depicting hemodynamic failure stages. For instance, in one study comparing arterial spin labeling versus (^{15}O-)H_2O-PET, normalization of the semiquantitative CBF values was done using perfusion values measured in the cerebellum to increase intermodality agreement.[7] For our data, however, this cannot be done because changes of cerebellar (-infratentorial-) perfusion reserve may differ from changes of the cerebral (-supratentorial-) perfusion reserve between the baseline and Diamox (^{15}O-)H_2O-PET scans, thereby leading to a higher variability (range) of values.

The current study was motivated by the ongoing effort to develop a standardized quantitative imaging method with potential wide clinical implementation to sensitively assess hemodynamic failure—and thereby stroke risk—in patients with chronic cerebrovascular steno-occlusive disease. Over the years, the noninvasive BOLD fMRI with standardized CO_2 has evolved into a quantitative technique to measure CVR on a high spatial resolution.[9,18,19] It can be easily implemented in routine clinical imaging, as well as prospective clinical trials investigating future stroke risk in patients with cerebrovascular steno-occlusive disease.

Clinical gold standard hemodynamic imaging techniques, such as PET and single photon emission CT, remain costly and have limited availability. The current development has, therefore, been focused on magnetic resonance–based techniques, such as magnetic resonance perfusion and arterial spin labeling. This development not only improves spatial imaging resolution and reduces the semiquantitative nature of

Downloaded from http://stroke.ahajournals.org/ by guest on July 19, 2018

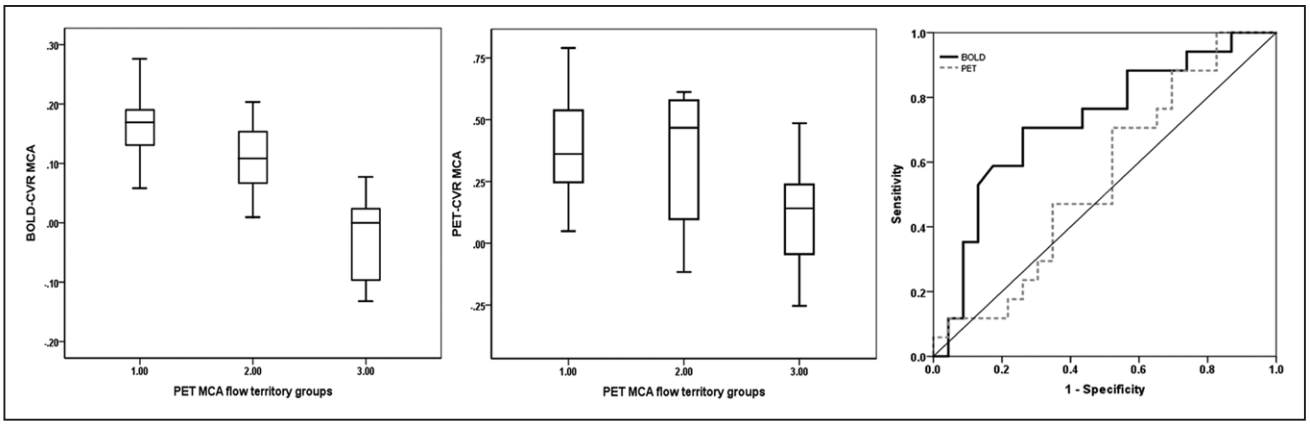

Figure 3. Correlation of hemodynamic failure staging of the middle cerebral artery (MCA) flow territory, blood oxygen-level–dependent (BOLD) vs positron emission tomography (PET). Box whisker plots depicting the distribution of quantitative BOLD CVR and PET perfusion reserve values for all 3 stage of hemodynamic failure within the MCA flow territory. Note that the distribution of the PET values is more widespread because of its semiquantitative determination and therefore weaker correlated. The receiver operating characteristic curve demonstrated an area under the curve of 0.73±0.08 for BOLD cerebrovascular reactivity (CVR) and 0.55±0.09 for PET perfusion reserve to detect hemodynamic failure stage II. Furthermore, a CVR cutoff value of 0.13 results in a 70% sensitivity and 74% specificity to detect hemodynamic failure stage 2.

these techniques but also aims for further standardization. For instance, Mutsaerts et al[20] asserted a strategy to develop comparable CBF maps by standardizing the arterial spin labeling protocol over multiple vendors and international centers to better determine a consensus on hemodynamic impairment. This idea may potentially strengthen the readout of any particular imaging modality. With BOLD CVR, a similar strategy has been proposed.[21,22] In this instance, standardization can even be better established because in addition to the BOLD fMRI sequence, the CO_2 stimulus is also standardized and reproducible.[9,23] For instance, the reproducibility analysis by Kassner et al[23] demonstrated excellent reproducibility for the within-day (intraclass correlation coefficient=0.92) and between-day (intraclass correlation coefficient=0.81) gray matter CVR estimates and good agreement for white matter CVR (intraclass correlation coefficient=0.88 and intraclass correlation coefficient=0.66, respectively). The quantitative CVR values derived from these standardized BOLD CVR studies can then be grouped specifically for either pathophysiology (eg, carotid artery occlusion), as well as for healthy subjects. By grouping BOLD CVR studies of healthy subjects, a healthy reference atlas can be created[18,22] that may assist in better determination of specific cutoff values for hemodynamic failure.

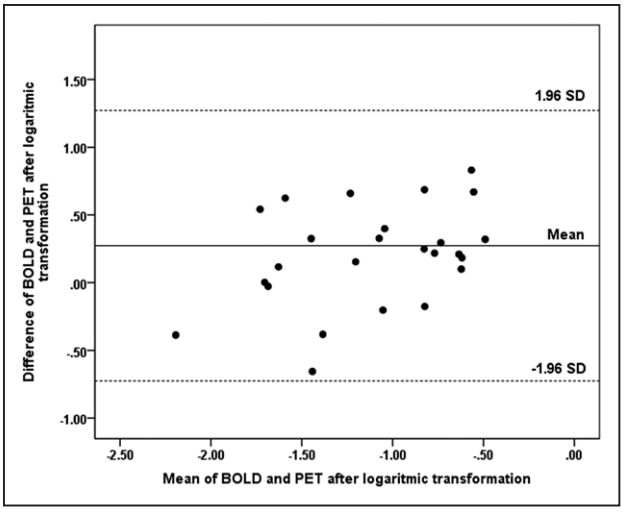

Figure 4. Limits of agreement between blood oxygen-level–dependent (BOLD) and positron emission tomography (PET). Bland–Altman plot to assess the limits of agreement between the 2 imaging techniques. Initially, a proportional bias was found (data not shown) which could be corrected for after logarithmic transformation (this figure).

Alternative Imaging Techniques to Assess Hemodynamic Failure and Stroke Risk

One of the most used parameters is oxygen extraction fraction. Powers et al[2,3] showed groundbreaking work and defined specific thresholds and stages of hemodynamic failure to predict stroke risk. A large prospective randomized trial based on these thresholds,[24] however, has challenged the robustness of the oxygen extraction fraction thresholds.[25] Impaired CVR measurements with Xenon-CT showed robust prediction of stroke risk, but this technique has no clinical role anymore in routine imaging.[26] Single photon emission CT, although experiencing similar limitations as PET on spatial resolution, costs, and limited clinical availability, has been another reliable technique to determine hemodynamic failure and stroke risk.[27] Transcranial Doppler remains a robust and widely clinical applicable screening tool but has low spatial resolution and and its flow measurement is not quantitative.[28,29] More recent magnetic resonance–based developments have put forward the use of multiparametric hemodynamic imaging, whereas parameters, such as mean transit time, cerebral metabolic rate of oxygen, cerebral blood volume either alone or in combination, are currently being investigated to determine a threshold for increased stroke risk.[30] CVR in response to CO_2[31–33] and Diamox[4,34] have been shown to be highly predictive of stroke.

Limitations

It can be argued that the patient population selected for this analysis is too heterogeneous. The main study objective, however, was to compare a novel imaging technique against the gold standard. Hence, the main inclusion criteria was

Downloaded from http://stroke.ahajournals.org/ by guest on July 19, 2018

unilateral hemodynamic failure determined with (^{15}O-)H_2O-PET and not a single cerebrovacular disease entity. This also led to enrollment of subjects that may have exhibited bilateral angiographic vascular disease but had only one hemodynamically impaired hemisphere. By selecting data sets with one affected and one unaffected hemisphere, the different hemodynamic patterns could be subsequently compared with BOLD CVR data.

Some specific limitations of the (^{15}O-)H_2O-PET technique are relevant to mention. Although the technique provides a direct CBF value, the true arterial input function is not measured. The arterial input function was derived from a healthy cohort (of young subjects) and is then assumed to have a similar shape in patients.[8] This may lead to misinterpretation of the data obtained within patient studies. This assumed arterial input function is also dependent on blood volume and cardiac output, where the lung blood pool is critical for the first dilution of the tracer in the body after intravenous infusion.

Finally, 2 different vasoactive stimuli were applied (ie, Diamox versus CO_2). Because we wanted to compare our novel technique of BOLD CO_2 CVR with the current clinical standard (15O-)H_2O-PET with Diamox, we opted to accept this difference, especially because the expected effect of both stimuli is maximal vasodilatation. Furthermore, work done by Ringelstein et al[28] and Ito et al[35] shows an excellent agreement between these 2 stimuli to measure intracranial CVR in patients with cerebrovascular steno-occlusive disease.

Future Directions

An important consideration would be the determination of universally defined thresholds to quantitatively identify the stages of hemodynamic failure. As mentioned previously, the groundwork for such has already been put in place (ie, standardization of BOLD CVR).[21,23] The next step is to create a reference atlas based on a large and age-stratified healthy population, as well as to implement the same protocol of this standardized BOLD CVR technique in various specialized centers to plan prospective studies on patients with chronic cerebrovascular steno-occlusive disease. A safety-analysis by Spano et al[11] has shown excellent feasibility of this technique within the clinical setting.

Conclusions

BOLD CVR compared with CBF perfusion reserve measurements obtained from (^{15}O-)H_2O-PET demonstrated a good agreement for hemodynamic failure in the affected hemisphere and MCA territory and for identifying hemodynamic failure stage II. BOLD CVR may, therefore, be considered for prospective studies assessing stroke risk in patients with chronic cerebrovascular steno-occlusive disease, in particular because it can potentially be widely implemented in routine clinical imaging.

Acknowledgments

We express our gratitude to the magnetic resonance technicians for enabling us to perform this study.

Sources of Funding

This research was supported by the Forschungskredit; Postdoc initiative 2016 from the University of Zurich allocated to Dr Fierstra (FK-16–040). Dr Warnock was funded by the Clinical Research Priority Program for Molecular Imaging of the University of Zurich (MINZ).

Disclosures

None.

References

1. Kamath A, Smith WS, Powers WJ, Cianfoni A, Chien JD, Videen T, et al. Perfusion CT compared to H(2) (15)O/O (15)O PET in patients with chronic cervical carotid artery occlusion. *Neuroradiology*. 2008;50:745–751. doi: 10.1007/s00234-008-0403-9.
2. Powers WJ. Cerebral hemodynamics in ischemic cerebrovascular disease. *Ann Neurol*. 1991;29:231–240. doi: 10.1002/ana.410290302.
3. Powers WJ, Press GA, Grubb RL Jr, Gado M, Raichle ME. The effect of hemodynamically significant carotid artery disease on the hemodynamic status of the cerebral circulation. *Ann Intern Med*. 1987;106:27–34.
4. Ogasawara K, Ogawa A, Terasaki K, Shimizu H, Tominaga T, Yoshimoto T. Use of cerebrovascular reactivity in patients with symptomatic major cerebral artery occlusion to predict 5-year outcome: comparison of xenon-133 and iodine-123-IMP single-photon emission computed tomography. *J Cereb Blood Flow Metab*. 2002;22:1142–1148. doi: 10.1097/00004647-200209000-00012.
5. Donahue MJ, Dethrage LM, Faraco CC, Jordan LC, Clemmons P, Singer R, et al. Routine clinical evaluation of cerebrovascular reserve capacity using carbogen in patients with intracranial stenosis. *Stroke*. 2014;45:2335–2341. doi: 10.1161/STROKEAHA.114.005975.
6. Mandell DM, Han JS, Poublanc J, Crawley AP, Stainsby JA, Fisher JA, et al. Mapping cerebrovascular reactivity using blood oxygen level-dependent MRI in Patients with arterial steno-occlusive disease: comparison with arterial spin labeling MRI. *Stroke*. 2008;39:2021–2028. doi: 10.1161/STROKEAHA.107.506709.
7. Kuhn FP, Warnock G, Schweingruber T, Sommerauer M, Buck A, Khan N. Quantitative H2[(15)O]-PET in pediatric Moyamoya disease: evaluating perfusion before and after cerebral revascularization. *J Stroke Cerebrovasc Dis*. 2015;24:965–971. doi: 10.1016/j.jstrokecerebrovasdis.2014.12.017.
8. Treyer V, Jobin M, Burger C, Teneggi V, Buck A. Quantitative cerebral H2(15)O perfusion PET without arterial blood sampling, a method based on washout rate. *Eur J Nucl Med Mol Imaging*. 2003;30:572–580. doi: 10.1007/s00259-002-1105-x.
9. Fierstra J, Sobczyk O, Battisti-Charbonney A, Mandell DM, Poublanc J, Crawley AP, et al. Measuring cerebrovascular reactivity: what stimulus to use? *J Physiol*. 2013;591:5809–5821. doi: 10.1113/jphysiol.2013.259150.
10. Mutch WA, Mandell DM, Fisher JA, Mikulis DJ, Crawley AP, Pucci O, et al. Approaches to brain stress testing: BOLD magnetic resonance imaging with computer-controlled delivery of carbon dioxide. *PLoS One*. 2012;7:e47443. doi: 10.1371/journal.pone.0047443.
11. Spano VR, Mandell DM, Poublanc J, Sam K, Battisti-Charbonney A, Pucci O, et al. CO2 blood oxygen level-dependent MR mapping of cerebrovascular reserve in a clinical population: safety, tolerability, and technical feasibility. *Radiology*. 2013;266:592–598. doi: 10.1148/radiol.12112795.
12. Alpert NM, Eriksson L, Chang JY, Bergstrom M, Litton JE, Correia JA, et al. Strategy for the measurement of regional cerebral blood flow using short-lived tracers and emission tomography. *J Cereb Blood Flow Metab*. 1984;4:28–34. doi: 10.1038/jcbfm.1984.4.
13. Slessarev M, Han J, Mardimae A, Prisman E, Preiss D, Volgyesi G, et al. Prospective targeting and control of end-tidal CO2 and O2 concentrations. *J Physiol*. 2007;581(pt 3):1207–1219. doi: 10.1113/jphysiol.2007.129395.
14. van Niftrik CHB, Piccirelli M, Bozinov O, Pangalu A, Fisher JA, Valavanis A, et al. Iterative analysis of cerebrovascular reactivity dynamic response by temporal decomposition. *Brain Behav*. 2017;7:e00705. doi: 10.1002/brb3.705.
15. Hammers A, Allom R, Koepp MJ, Free SL, Myers R, Lemieux L, et al. Three-dimensional maximum probability atlas of the human brain,

Downloaded from http://stroke.ahajournals.org/ by guest on July 19, 2018

with particular reference to the temporal lobe. *Hum Brain Mapp*. 2003;19:224–247. doi: 10.1002/hbm.10123.
16. Fierstra J, Poublanc J, Han JS, Silver F, Tymianski M, Crawley AP, et al. Steal physiology is spatially associated with cortical thinning. *J Neurol Neurosurg Psychiatry*. 2010;81:290–293. doi: 10.1136/jnnp.2009.188078.
17. Conklin J, Fierstra J, Crawley AP, Han JS, Poublanc J, Mandell DM, et al. Impaired cerebrovascular reactivity with steal phenomenon is associated with increased diffusion in white matter of patients with Moyamoya disease. *Stroke*. 2010;41:1610–1616. doi: 10.1161/STROKEAHA.110.579540.
18. Blockley NP, Jiang L, Gardener AG, Ludman CN, Francis ST, Gowland PA. Field strength dependence of R1 and R2* relaxivities of human whole blood to ProHance, Vasovist, and deoxyhemoglobin. *Magn Reson Med*. 2008;60:1313–1320. doi: 10.1002/mrm.21792.
19. Fierstra J, Conklin J, Krings T, Slessarev M, Han JS, Fisher JA, et al. Impaired peri-nidal cerebrovascular reserve in seizure patients with brain arteriovenous malformations. *Brain*. 2011;134(pt 1):100–109. doi: 10.1093/brain/awq286.
20. Mutsaerts HJ, van Osch MJ, Zelaya FO, Wang DJ, Nordhøy W, Wang Y, et al. Multi-vendor reliability of arterial spin labeling perfusion MRI using a near-identical sequence: implications for multi-center studies. *Neuroimage*. 2015;113:143–152. doi: 10.1016/j.neuroimage.2015.03.043.
21. Sobczyk O, Battisti-Charbonney A, Fierstra J, Mandell DM, Poublanc J, Crawley AP, et al. A conceptual model for CO_2-induced redistribution of cerebral blood flow with experimental confirmation using BOLD MRI. *Neuroimage*. 2014;92:56–68. doi: 10.1016/j.neuroimage.2014.01.051.
22. Sobczyk O, Battisti-Charbonney A, Poublanc J, Crawley AP, Sam K, Fierstra J, et al. Assessing cerebrovascular reactivity abnormality by comparison to a reference atlas. *J Cereb Blood Flow Metab*. 2015;35:213–220. doi: 10.1038/jcbfm.2014.184.
23. Kassner A, Winter JD, Poublanc J, Mikulis DJ, Crawley AP. Blood-oxygen level dependent MRI measures of cerebrovascular reactivity using a controlled respiratory challenge: reproducibility and gender differences. *J Magn Reson Imaging*. 2010;31:298–304. doi: 10.1002/jmri.22044.
24. Powers WJ, Clarke WR, Grubb RL Jr, Videen TO, Adams HP Jr, Derdeyn CP; COSS Investigators. Extracranial-intracranial bypass surgery for stroke prevention in hemodynamic cerebral ischemia: the Carotid Occlusion Surgery Study randomized trial. *JAMA*. 2011;306:1983–1992. doi: 10.1001/jama.2011.1610.
25. Carlson AP, Yonas H, Chang YF, Nemoto EM. Failure of cerebral hemodynamic selection in general or of specific positron emission tomography methodology?: Carotid Occlusion Surgery Study (COSS). *Stroke*. 2011;42:3637–3639. doi: 10.1161/STROKEAHA.111.627745.
26. Yonas H, Smith HA, Durham SR, Pentheny SL, Johnson DW. Increased stroke risk predicted by compromised cerebral blood flow reactivity. *J Neurosurg*. 1993;79:483–489. doi: 10.3171/jns.1993.79.4.0483.
27. Hokari M, Kuroda S, Shiga T, Nakayama N, Tamaki N, Iwasaki Y. Impact of oxygen extraction fraction on long-term prognosis in patients with reduced blood flow and vasoreactivity because of occlusive carotid artery disease. *Surg Neurol*. 2009;71:532–538; discussion 538. doi: 10.1016/j.surneu.2008.02.033.
28. Ringelstein EB, Kahlscheuer B, Niggemeyer E, Otis SM. Transcranial Doppler sonography: anatomical landmarks and normal velocity values. *Ultrasound Med Biol*. 1990;16:745–761.
29. Schneider J, Sick B, Luft AR, Wegener S. Ultrasound and clinical predictors of recurrent ischemia in symptomatic internal carotid artery occlusion. *Stroke*. 2015;46:3274–3276. doi: 10.1161/STROKEAHA.115.011269.
30. Grubb RL Jr, Derdeyn CP, Videen TO, Carpenter DA, Powers WJ. Relative mean transit time predicts subsequent stroke in symptomatic carotid occlusion. *J Stroke Cerebrovasc Dis*. 2016;25:1421–1424. doi: 10.1016/j.jstrokecerebrovasdis.2015.12.041.
31. Silvestrini M, Vernieri F, Pasqualetti P, Matteis M, Passarelli F, Troisi A, et al. Impaired cerebral vasoreactivity and risk of stroke in patients with asymptomatic carotid artery stenosis. *JAMA Neurol*. 2000;283:2122–2127.
32. Kleiser B, Krapf H, Widder B. Carbon dioxide reactivity and patterns of cerebral infarction in patients with carotid artery occlusion. *J Neurol*. 1991;238:392–394.
33. Markus H, Cullinane M. Severely impaired cerebrovascular reactivity predicts stroke and TIA risk in patients with carotid artery stenosis and occlusion. *Brain*. 2001;124(pt 3):457–467.
34. Kuroda S, Houkin K, Kamiyama H, Mitsumori K, Iwasaki Y, Abe H. Long-term prognosis of medically treated patients with internal carotid or middle cerebral artery occlusion: can acetazolamide test predict it? *Stroke*. 2001;32:2110–2116.
35. Ito S, Mardimae A, Han J, Duffin J, Wells G, Fedorko L, et al. Non-invasive prospective targeting of arterial P(CO2) in subjects at rest. *J Physiol*. 2008;586:3675–3682. doi: 10.1113/jphysiol.2008.154716.

Stroke
American Heart Association | American Stroke Association
Downloaded from http://stroke.ahajournals.org/ by guest on July 19, 2018

Stroke
Journal of the American Heart Association

American Heart Association | American Stroke Association

Staging Hemodynamic Failure With Blood Oxygen-Level–Dependent Functional Magnetic Resonance Imaging Cerebrovascular Reactivity: A Comparison Versus Gold Standard (15O-)H2O-Positron Emission Tomography

Jorn Fierstra, Christiaan van Niftrik, Geoffrey Warnock, Susanne Wegener, Marco Piccirelli, Athina Pangalu, Giuseppe Esposito, Antonios Valavanis, Alfred Buck, Andreas Luft, Oliver Bozinov and Luca Regli

Stroke. published online January 25, 2018;
Stroke is published by the American Heart Association, 7272 Greenville Avenue, Dallas, TX 75231
Copyright © 2018 American Heart Association, Inc. All rights reserved.
Print ISSN: 0039-2499. Online ISSN: 1524-4628

The online version of this article, along with updated information and services, is located on the World Wide Web at:
http://stroke.ahajournals.org/content/early/2018/01/23/STROKEAHA.117.020010

Data Supplement (unedited) at:
http://stroke.ahajournals.org/content/suppl/2018/02/13/STROKEAHA.117.020010.DC1

Permissions: Requests for permissions to reproduce figures, tables, or portions of articles originally published in *Stroke* can be obtained via RightsLink, a service of the Copyright Clearance Center, not the Editorial Office. Once the online version of the published article for which permission is being requested is located, click Request Permissions in the middle column of the Web page under Services. Further information about this process is available in the Permissions and Rights Question and Answer document.

Reprints: Information about reprints can be found online at:
http://www.lww.com/reprints

Subscriptions: Information about subscribing to *Stroke* is online at:
http://stroke.ahajournals.org//subscriptions/

Downloaded from http://stroke.ahajournals.org/ by guest on July 19, 2018